Drilling of Graphite/Bismaleimide Composite Material

M. Ramulu, P. Young, and H. Kao

(Submitted 17 July 1997; in revised form 1 February 1999)

Drilling study of graphite/bismaleimide composite material was conducted by using different cutter materials (high-speed steel, carbide, and polycrystalline diamond) and drill geometries. It was found that polycrystalline diamond tools outperformed all other tools in terms of minimal surface damage, delamination, and fiber pullout. The drilling forces exerted in machining graphite/bismaleimide were recorded by using a dynamometer, and the morphology of drilled surfaces was evaluated with surface profilometry and optical and scanning electron microscopy. The drilling characteristics were evaluated in terms of cutting forces, tool wear, and surface morphology.

Keywords Bismaleimide, diamonds, fiber reinforced plastic, graphite, joining

1. Introduction

Development of fiber reinforced plastics (FRPs) within the past few decades has enabled the use of lighter, stronger component parts in a variety of engineering structures. High strength-to-weight ratios, high stiffness qualities, excellent corrosion resistance, and excellent fatigue properties have led to their use in many other industries as well. The diverse range of products manufactured from composites includes bicycle frames, tennis rackets, and computer circuit boards, not to mention various aerospace and automotive uses. Graphite/bismaleimide (Gr/Bi) is one of the FRP materials used in the aerospace industry and is most commonly manufactured into preshaped or preformed components. However, for joining and assembling, secondary machining processes such as drilling and edge trimming are required. Unfortunately, edge machining of composites often leads to edge delamination in the machined region, severe reduction in the load carrying capacity, and reduction in stiffness of the component (Ref 1).

Drilling is often the last manufacturing process to be conducted on a part before assembly. Because of difficulty in machining of FRPs, quality hole production is a challenging task for manufacturing engineers.

Unlike drilling homogenous materials, drilling of fiber reinforced materials allows for the possibility of many defects, such as delamination, microcracking, debonding, and fiber pullout (Ref 2, 3). The most prevalent hole defect is exit delamination (Ref 4). Therefore, it is important to understand the drilling process in FRPs for quality hole making.

The cutting mechanisms of FRPs have been investigated in orthogonal trimming of unidirectional laminate materials by several researchers (Ref 5-9). Machining forces, ply delamination, and tool wear were investigated in early orthogonal studies. It was found that the machining damage depended on the fiber directions and the laminate stacking sequence (Ref 2, 7, 9). Recently, the authors (Ref 9-13) and others (Ref 14-18) have investigated cutting mechanisms based on new tooling types and geometries, which were designed and evaluated. The results of these studies have been varied, and they were found to depend on the materials being machined. However, there was no research reported about Gr/Bi materials either on machining or drilling.

The purpose of this study was to investigate the drilling characteristics of Gr/Bi composite material. Commercially available, industry-recommended drill bit geometries made from high-speed steel (HSS), carbide, and polycrystalline diamond (PCD) were used. The drilling characteristics are reported in terms of cutting forces, tool wear, and surface finish.

2. Experimental Setup and Procedure

2.1 Materials

The FRP material used in this investigation was multidirectional IM715260 graphite/bismaleimide composite (Gr/Bi), which was acquired from the Boeing Company. The Gr/Bi material strips were nominally 4 mm thick and approximately 0.5 m long. Ply thickness was 0.178 mm and ply orientation was $[45/90/-45/0/-45/0/45/0/45/-45/90/90]_s$ bisected by a centerline of three plies at 90° orientation. The drilling tools used in this investigation were produced from three main material

M. Ramulu, P. Young, and **H. Kao,** Department of Mechanical Engineering, Box 352600, University of Washington, Seattle, WA 98195-2600, USA.

Table 1 Drill tool geometries

Drill	Diameter, mm	Point angle, degrees	Relief angle, degrees	Rake angle, degrees
HSS drill	6.35	118	15	33
Carbide straight Flute drill	5.54	primary 118 secondary 17	primary 10 secondary 19	primary 17 secondary 5
PCD drill	6.35	118	primary 15 secondary 25	7

types, namely high-speed steel (HSS), carbide, and polycrystalline diamond (PCD). Drill geometries are listed in Table 1 and shown in Fig. 1.

2.2 Machine Tool Setup, Tooling, and Procedure

A Bridgeport vertical mill that had been retrofitted with a CNC control and drive unit was utilized to machine the test specimens. The servomotors of the mill were programmable for different feed rates, with a capability of four spindle speeds (between 660 and 2720 rpm) during the Gr/Bi drilling tests.

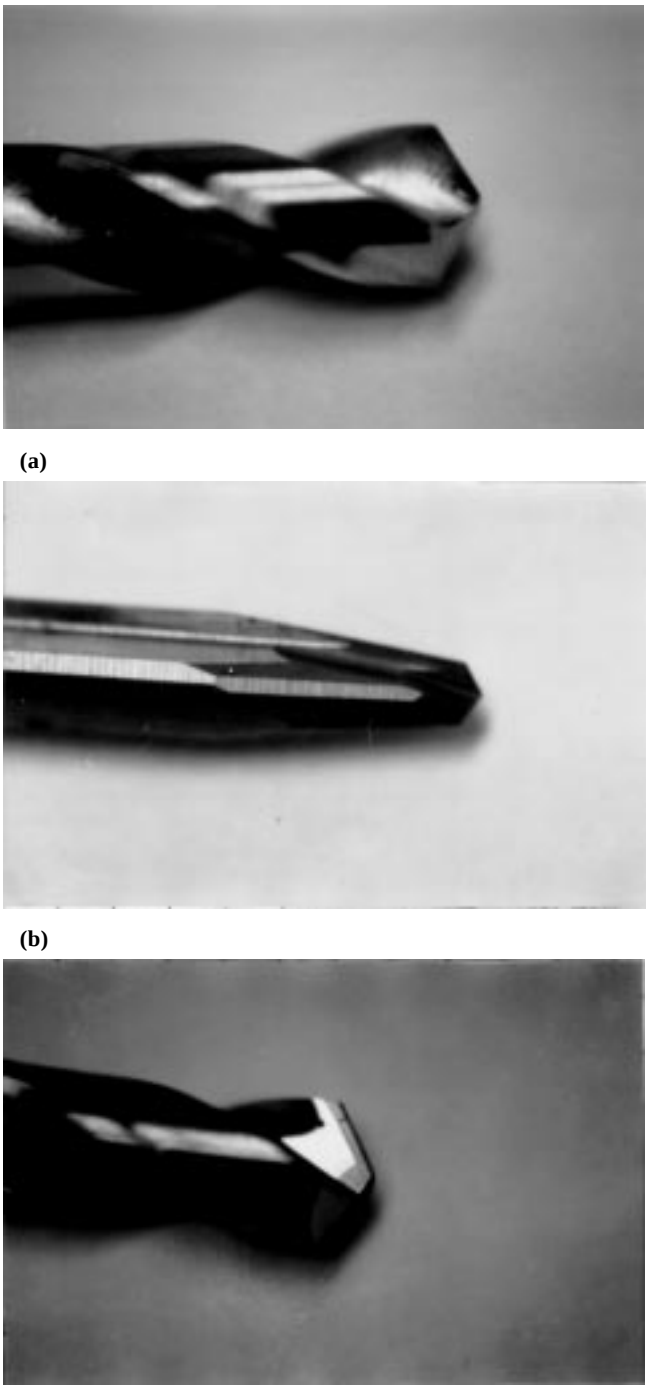

(a)

(b)

(c)

Fig. 1 Drilling tools. (a) High-speed steel (HSS) drill. (b) Carbide Dagger drill. (c) Polycrystalline diamond (PCD) drill

Tools used included three types of drills. The specialized drill types were chosen because they are currently in use by many major aerospace manufacturers. The HSS drill is the typical drill used for mild steels and is readily available through many different suppliers. The Dagger (also known as four-flute tapered, straight flute drill/reamer; Grobet USA, Carlstadt, NJ) drill design differs in that it has primary, secondary, and tertiary cutting zones, with the first zone being much like that of a small conventional drill. The second cutting section increases the hole size from the diameter of the small tip to that of the third cutting zone by engaging the workpiece with four cutting edges. The third cutting area is a four-flute reamer, which finishes the hole to the desired diameter. The PCD drill is a four-facet drill with a true cutting point at the tip of the drill. The four facets meet at the very tip of the tool to engage cutting action rather than extrusion as with typical geometry, cam-relief ground drills.

A schematic of the test setup can be seen in Fig. 2, and the actual setup of machining of the test apparatus is shown in Fig. 3(a), with a close-up of the dynamometer setup in Fig. 3(b). The summary of experimental conditions is listed in Table 2. The system was designed to accommodate a drilling dynamometer, which was equipped with strain gages. This cylinder of aluminum was fitted with two sets of strain gages, which were aligned to be independently sensitive to torque and thrust forces applied to the dynamometer. Two amplifiers were used

Table 2 Summary of experimental conditions

Component	Description
Machine	Bridgeport vertical mill with CNC control
Drills	HSS drill, 6.35 mm diameter
	Carbide straight flute drill, 5.45 mm diameter
	PCD drill, 6.35 mm diameter
Drilling parameters	Drilling speeds: 660, 1320, and 2720 rpm
	Feed rate: 0.028 mm/rev
Workpiece material	IM715260 graphite bismaleimide composite (Gr/Bi)

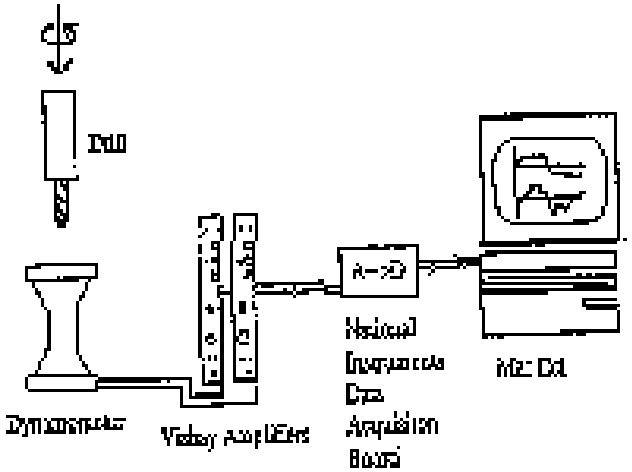

Fig. 2 Schematic of drilling data acquisition system

to supply the strain gages with a small voltage, to balance the Wheatstone bridge circuit, and to amplify the output signal from the circuit to ±10 V. A commercially available data acquisition software was used to analyze the force signals and record the drilling force data.

2.3 Experimental Design and Analysis

The experiments were designed to investigate the relationships between different tools and drilling forces in Gr/Bi. The first set of experiments was conducted to study the effects of different drill bit geometries and materials on the cutting forces, tool wear, and hole quality; several different cutting tools were evaluated at the constant drilling parameters of 2720 rpm and 0.028 mm/rev. The second set of drilling experiments was conducted at the three speed levels 660, 1320, and 2720 rpm. All holes were drilled at the feed rate 0.028 mm/rev. Drilled specimens were analyzed by optically measuring delamination at the exit ply.

Delamination was defined to be any area of the exit ply originating at the hole edge and protruding below the plane of the edge of the material. The hole diameter was subtracted from the total distance of delamination.

(a)

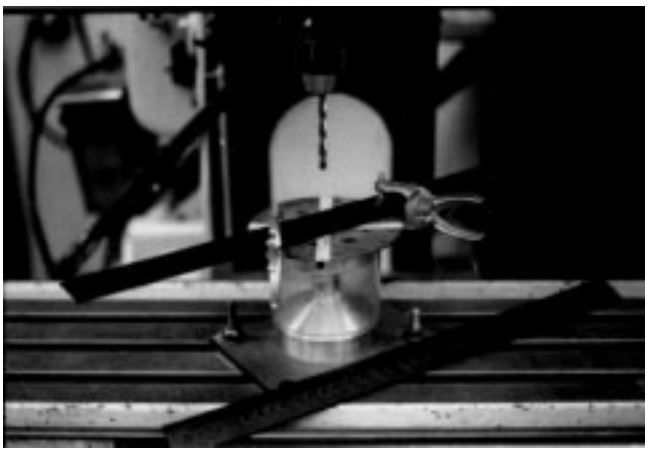

(b)

Fig. 3 Actual setup of machining apparatus. (a) Testing setup. (b) Drill dynamometer and drilled specimen

To evaluate the hole quality, the surface roughness across the depth of the hole walls was measured on a Surfanalyzer System 4000 (Federal Products Co., Providence, RI) with an EPT-01049 diamond stylus probe, 2.54 μm radius. All the surface profiles were recorded with a cutoff length of 0.8 mm, a drive speed of 0.25 mm/s, and a traverse length of 3.9 mm. The recorded surface roughness profiles were used to calculate the surface characterizing parameters such as average roughness, R_a; the maximum peak-to-valley height, R_y; the root mean square average, R_q; and the ten point average roughness, R_z; by using a surface roughness analysis (SRA) program developed at the University of Washington and described in detail in Ref 18. Selected specimens were cut and sectioned so as to investigate the hole wall surface characteristics.

A Jeoul JSM-T300A scanning electron microscope (SEM) was used to qualitatively evaluate the microstructure surface intensity of the sectioned hole walls. At low magnification levels of 35×, the exit delamination and gross hole quality were examined, and the surface and damages of the cut surfaces were evaluated at higher magnifications. Optical microscopy was utilized in measuring the amount of flank wear of the drills.

3. Results and Discussion

Typical drilled hole configurations using three different tools are shown in Fig. 4. Figure 4(a) shows an example of entrance delamination produced with the HSS drill, and Fig. 4(b) is the side view of those two holes shown in Fig. 4(a). In Fig. 4(c) the top view of holes drilled with the Dagger drill can be seen, and one can find that the rough, loose fibers of the HSS hole have been replaced with closely cropped fibers producing a much smoother finish. The PCD produced the holes without delamination as shown in Fig. 4(d).

3.1 Drilling Forces

Thrust force and the torque recorded for the holes drilled at constant cutting conditions of 0.028 mm/rev feed and a speed of 2720 rpm by HSS, carbide, and PCD tools are shown in Fig. 5. Figure 5(a) shows the penetration of the drill tip into the workpiece at the time of approximately 1.2 s and full engagement of the cutting edges at 2.5 s. The tool tip penetrates the workpiece at 4.5 s followed by a quick decrease in the thrust force as more of the length of the cutting edges passes the final ply of the composite. At 5.5 s the tool is no longer cutting but is still traversing through the workpiece, with the helical flutes or grooves of the drill imparting a pulling force on the workpiece. This can be seen as a positive thrust force from 5.5 to 7.5 s at which the tool is rapidly retracted out of the work, resulting in no net forces.

The torque can be seen to reach its maximum at the point when the tip of the tool passes through the last ply, with subsequent cutting action taking place on less than the entire cutting edge of the drill. The maximum thrust force can be seen to occur approximately 0.1 s after the tool engages the workpiece, or at a hole depth of 0.130 mm. The torque can be seen to fail to return directly to zero after the penetration of the drill tip in the work. This might be due to the very fine chips and dust from the specimen being forced upward through the drill flutes. These

small Gr/Bi chips and dust become wedged between the tool and workpiece, therefore continuing to induce a torque force after the cutting action has finished.

Figure 5(b) shows the drilling forces for the third, fourth, and fifth holes drilled by the 5.54 mm carbide Dagger drill. At point 1, the tip of the tool has impacted the workpiece, and the large point angle of this section of the drill leads to relatively large thrust forces. Between points 1 and 2, the second section of the drill engages the work, increasing the thrust and torque forces. At point 2 the tip passes through the work with the thrust force reaching its peak value. The less-abrupt second section is still engaging the work, and the lower thrust force of 30 N can be attributed solely to that second section.

Note that the thrust decreases gradually from points 3 to 4 as more and more of the secondary cutting edges pass through the work. At point 4 the cutting edges have passed completely through the work, but the thrust and torque forces persist at lower values due to the continued travel of the tool and the lesser engagement of the flutes and the work. The workpiece has stray fibers that protrude from the edge into the hole, and these fibers are acted upon by the revolving flutes. At point 5 the tool rapidly passes back through the work, leaving the forces at zero. It is interesting to see that the maximum thrust force magnitude is much smaller (with the carbide Dagger drill) than it is with the HSS tools.

Figure 5(c) shows the torque and thrust force recorded with PCD drill. A spike in the torque curve can be seen at the point at which the tip of the tool passed through the last composite ply, and the ensuing decrease in the thrust value as the tool finished its travel. Note that the drill point angle, cutting edge angle shape, and design (including the smaller web thickness) of the PCD drill are similar to those of the HSS drill, but the PCD drill induced thrust forces approximately one third of the thrust forces of the HSS tool. The four-facet drill tip design allows the tool to cut the workpiece with the tip of the tool, not to push and extrude the material, resulting in lower thrust forces. The PCD drill caused the lowest thrust forces of any tool tested.

Figure 6 shows the thrust force measurements made in drilling Gr/Bi material. Holes were drilled at the constant cutting conditions of speed 2720 rpm and feed 0.02794 mm/rev for the HSS and PCD drills. Increase of thrust force can be seen to be insignificant for the PCD tool when compared to the thrust force increase in HSS tool. The HSS drill induced thrust forces initially of around 150 N with subsequent holes producing

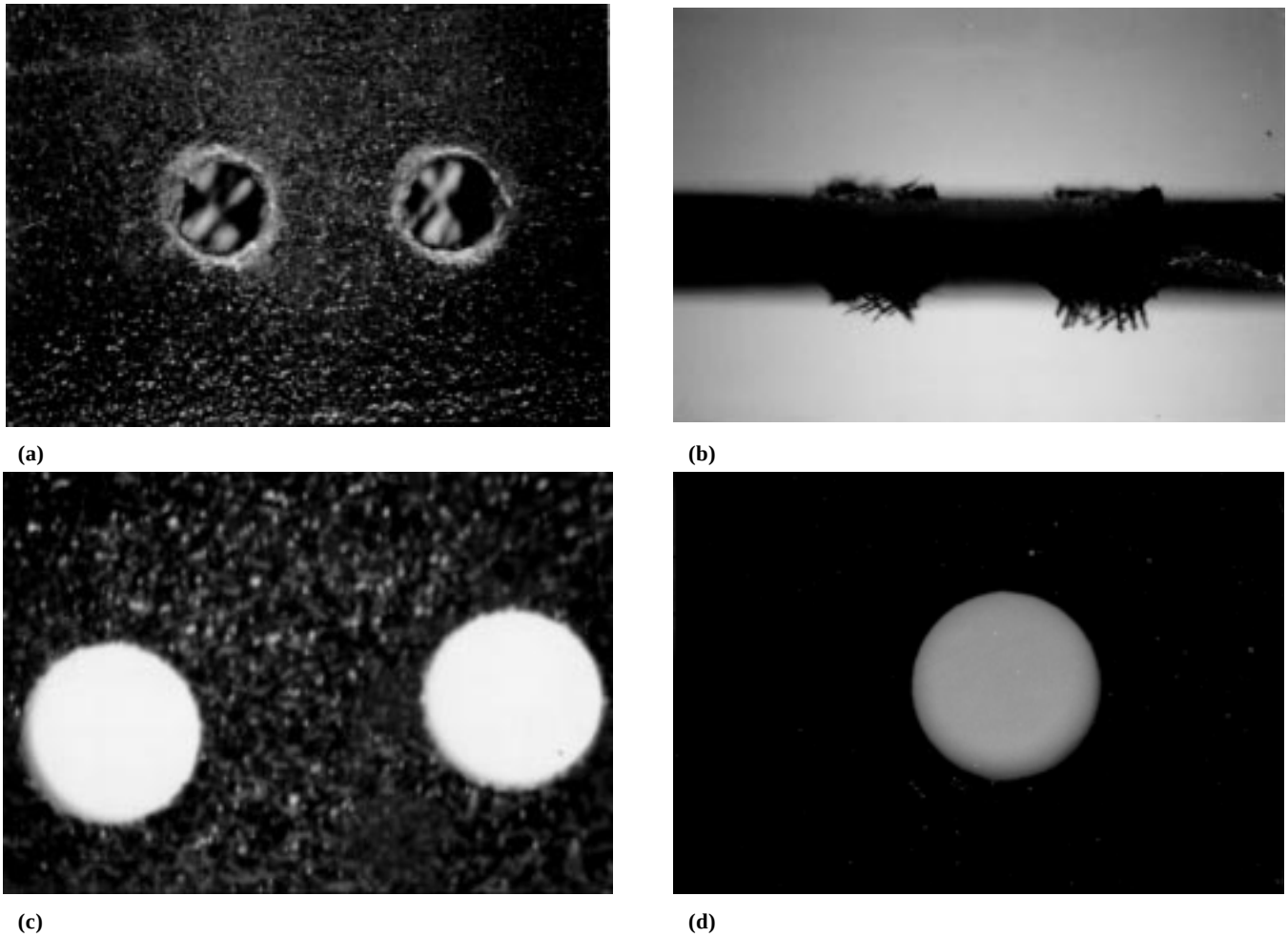

Fig. 4 Drilled hole configurations. (a) Top view of eighth and ninth holes drilled with HSS drill. (b) Entrance delamination (side view) of eighth and ninth holes drilled with HSS drill. (c) Top view of holes drilled with carbide Dagger drill. (d) Top view of hole drilled with PCD drill

thrusts of 450 N. Burning of the composite occurred during the drilling of the 15th hole and continued during each subsequent hole, until the HSS drill failed after 20 holes. The PCD drill, however induced only 50 N on its first hole and less than 100 N after drilling 40 holes. After drilling 40 holes, a PCD drill induced one half the thrust force of a new HSS drill. It is not surprising that the PCD drill has the highest hardness of any of the tool materials, and consequently it best resisted wear.

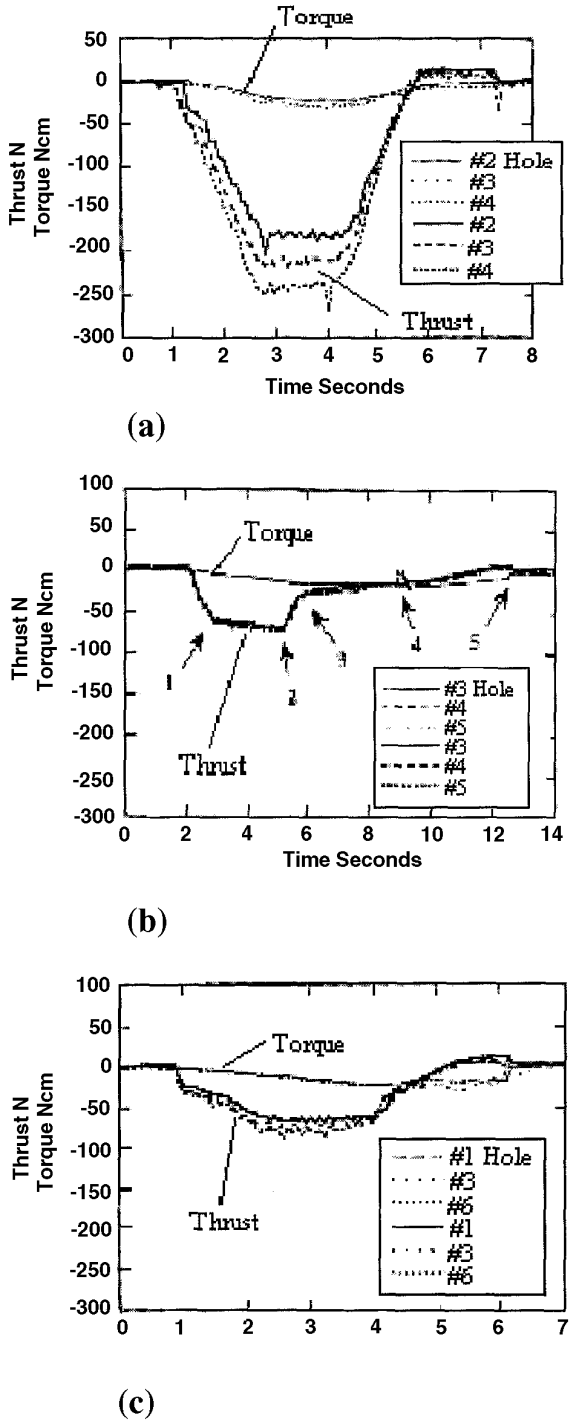

Fig. 5 Drilling forces at 2720 rpm and 0.028 mm/rev. (a) HSS drill. (b) Carbide Dagger drill. (c) Polycrystalline diamond drill

3.2 Tool Wear

During the drilling of the highly abrasive Gr/Bi, HSS tools suffered the most from wear of their cutting edges and flank faces. Figure 7 shows both the flank wear and the thrust forces, at three speed levels and at a constant feed of 0.0028 mm/rev, for new HSS drills over the first 20 holes that the tools machined. The slower speeds resulted in higher wear rates at the

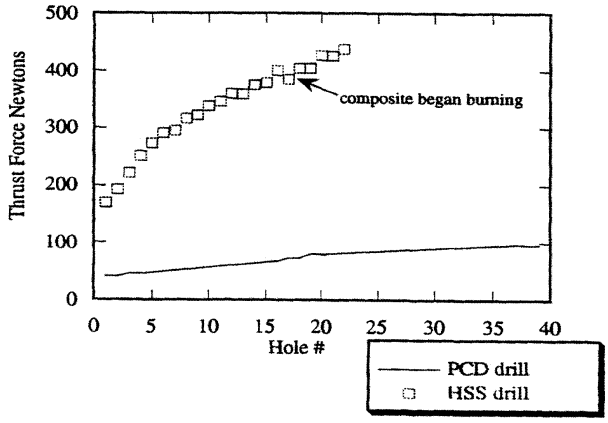

Fig. 6 Thrust force versus number of holes drilled, 2720 rpm and 0.028 mm/rev

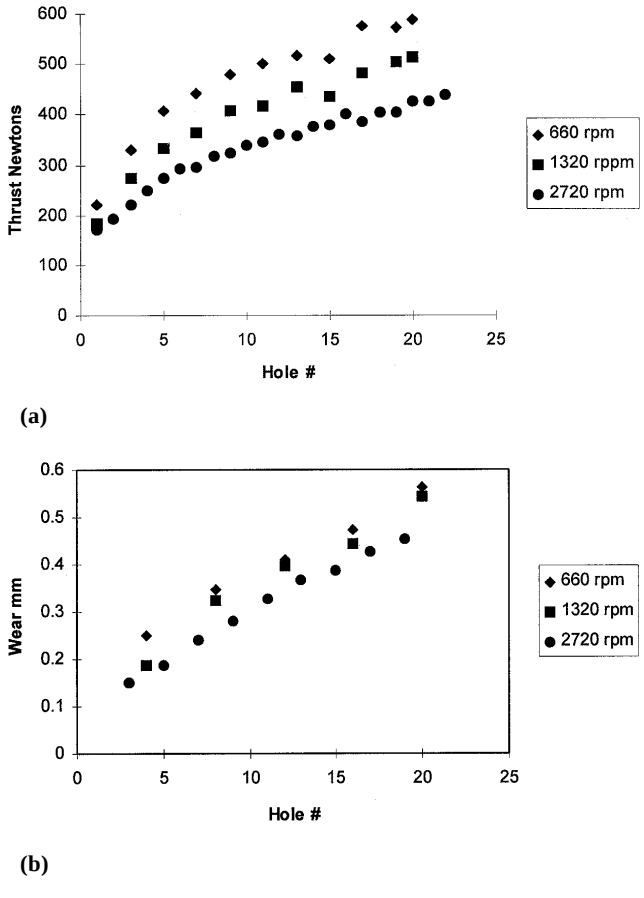

Fig. 7 Thrust force and flank wear of HSS drill over first 20 holes. (a) Thrust force versus hole number. (b) Wear versus hole number

same feed, due to longer engagement times between the tool and the workpiece. Longer machining times led to higher abrasion, due to the fibers rubbing on the tool. This action increased wear, and consequently the fibers were cut less cleanly, leaving more fibers to rub on the tool. The difference in tool wear can account for the increase in thrust force, as the new tools at each speed produced similar thrusts. The lower speeds quickly wore the tools and the thrust increased over the baseline 2720 rpm case. Hole quality for all three speeds was poor after the first, with entrance and exit delamination, matrix burning, and many uncut fibers protruding into the hole area.

Delamination and tool wear were found to be concerns when drilling Gr/Bi. Due to the abrasive graphite fibers, HSS tooling suffered large amounts of abrasive wear, while carbide and PCD tooling were found to wear less than 50 μm and 5 μm respectively. Tool life for HSS tools was less than one hole, with the first hole drilled being above the critical thrust force of 100 N and producing exit (and entrance) delamination. Continued use of worn HSS drills resulted in increasing damage to the hole wall. Therefore HSS tools are not recommended for use in this material. Polycrystalline diamond tooling was found to produce holes of better quality.

3.3 Surface Topography

The surface roughness of the third hole drilled by the HSS drill can be seen in Fig. 8(a), with the exit ply being represented on the rightmost portion of the graph and the entrance ply being represented on the left. Note that the traverse length is approximately 3500 μm or 3.5 mm. This length was chosen so as to cover the majority of the specimen thickness of approximately 5 mm, with the entrance plies not being analyzed by the profilometer. The surface roughness of 23 HSS drilled holes used in the wear study (drilled at 2720 rpm) were measured, and the third and 23rd hole surface profiles are shown in Fig. 8(a and b) respectively. The R_a value increases from 5 to 20 μm over the first dozen holes drilled. Tool wear can be directly seen then to negatively influence the hole quality substantially from the beginning of the use of a tool. Surface roughness data for the first hole is given in Table 3 for three different drills. R_a is the average roughness, R_q is the root-mean-squared height, R_y is the maximum peak-to-valley height, and R_z is the ten-point height. The R_y value was about 8 to 10 times the R_a value regardless of the tool material. The four-facet cutting of the PCD drill enabled the drill to cut through the specimen cleanly without in-

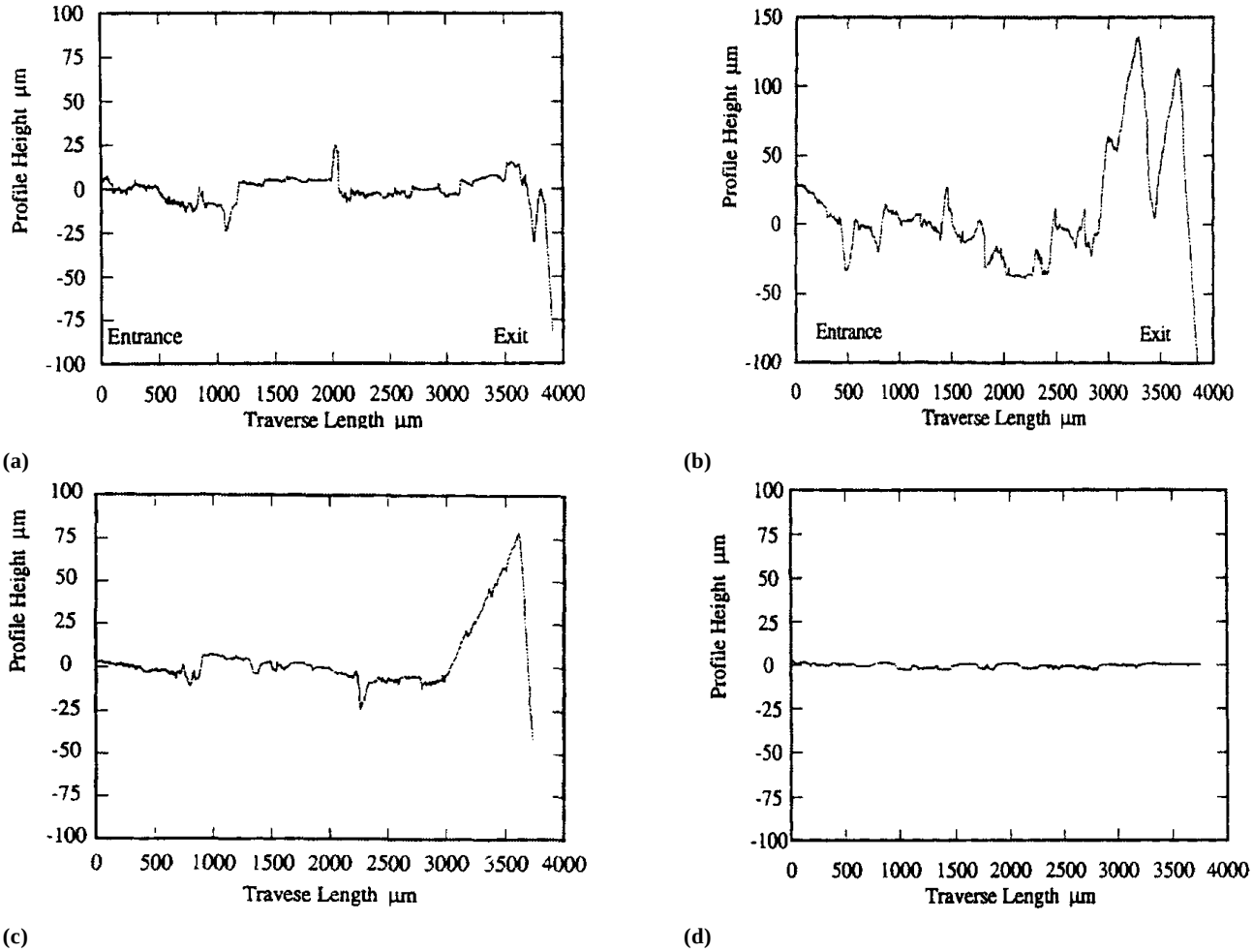

Fig. 8 Surface profile (all holes drilled at 2720 rpm and 0.028 mm/rev). (a) Surface profile of third hole drilled with HSS drill. (b) Profile of 23rd hole drilled by HSS tool. (c) Surface profile of hole drilled with carbide Dagger drill. (d) Surface profile of hole drilled with PCD tool

ducing surface flaws such as pitting or matrix smearing. In comparison to the hole produced by the worn HSS drill, the surface of the hole produced by the carbide dagger drill can be seen as an improvement (Fig. 8c). Consequently, the roughness values for the PCD drill are significantly better than those for the other drills (Fig. 8d). The HSS seemed to produce holes with lower roughness heights than those produced by the carbide drill initially, but the tenth hole produced by the HSS drill was found to be of higher roughness than those produced by the carbide drill.

The amount of exit delamination is also tabulated in Table 3, and the HSS drill, at 4.42 mm, is the only tool that produced measurable delamination. The HSS drill initially produced holes with little delamination in the as-received condition of the drill. Figure 9 shows the value of exit delamination when HSS drilled Gr/Bi at a speed of 2720 rpm and a feed of 0.028 mm/rev. After drilling as few as one to two holes, the drill induced delamination at the entrance and exit plies and produced rough hole wall surfaces. The HSS drilling bits with conventional helical grooves can be seen to impart pulling thrust forces on the workpiece after fully penetrating the work. A strong correlation between the amount of tool wear and the hole quality was observed as shown in Fig. 10. Cutting conditions used in this series of experiments are at the speed of 2720 rpm and feed of 0.028 mm/rev.

Table 3 Hole surface roughness parameters and exit delamination for first hole by each drill type (2720 rpm, 0.028 mm/rev, Gr/Bi)

	Drill materials		
Parameter, μm	**HSS**	**Carbide**	**PCD**
R_a, μm	5.24	8.22	1.13
R_q, μm	7.38	15.61	1.45
R_y, μm	50.76	98.67	7.27
R_z, μm	30.96	80.29	6.66
Delamination, mm	4.42	0	0

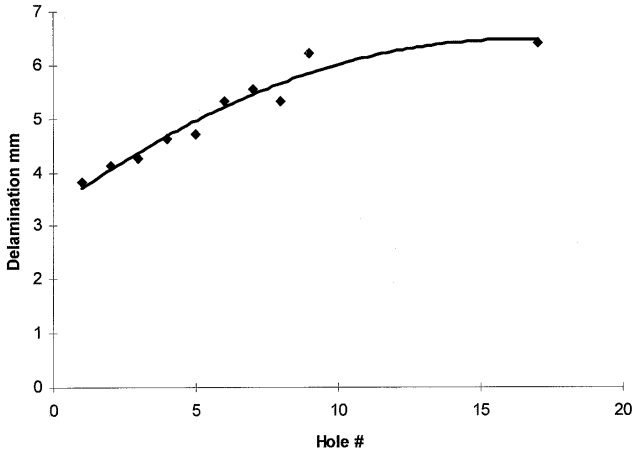

Fig. 9 Delamination versus hole number, HSS drill 2720 rpm, 0.028 mm/rev

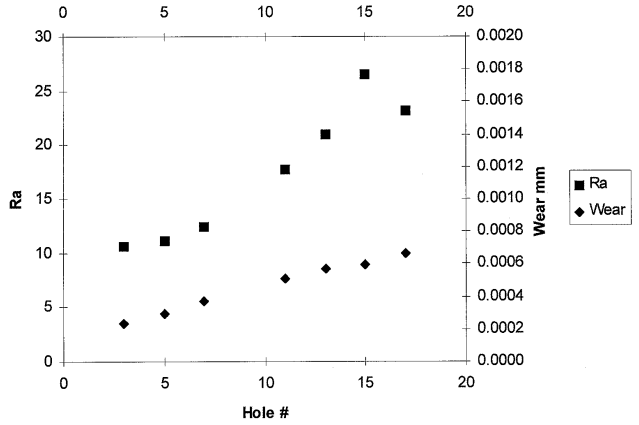

Fig. 10 Flank wear and R_a versus hole number of holes drilled by HSS drill, 2720 rpm, 0.028 mm/rev

Figure 11(a) is a SEM micrograph of the last two plies of a delaminated hole. An SEM micrograph of the sectioned hole wall is shown in Fig. 11(b), with considerable uncut fibers and a poor surface finish. Matrix burning and smearing was a problem with the HSS drill, especially as the tool began to wear. In Fig. 11(c), a section of a hole is seen to contain a large area of burned matrix and loose fiber ends. The high heat associated with cutting using a worn tool caused the matrix to melt and to capture many of the loose cut fibers. This material flowed down the cut surface of the hole, cooled, solidified and left the uneven and weak surface seen in the figure. At high magnifications, the machined area can be seen to contain many small fiber bits in random orientations, providing little (if any) strength to the specimen. The hole surface drilled by carbide Dagger can be seen in the SEM micrograph of Fig. 12(a). Some matrix burning is apparent, and a few stray fibers appear not to have been cut, or they have been pulled out of the cut surface. A small amount of pitting was observed with the PCD, and this is photographed in Fig. 12(b). The amount of pitting by the PCD was very minimal compared to the extensive pitting and other gross damage done to the specimens by the HSS drill. Figure 12(c) is an SEM micrograph that shows the very clean-cut surface produced by the PCD drill in comparison to the cut surfaces produced by the other two drills.

4. Conclusions

Experimental study of drilling holes in Gr/Bi composite material was conducted by using different tools and different tool materials and geometries. Based on this study, the following conclusions were made:

- The PCD four-facet drill produced the highest quality holes and suffered the least amount of wear.
- With high degrees of abrasive wear experienced by the tools, wear-resistant, harder tools are required. Tool geometry must be designed and chosen so as to minimize the amount of hole damage in the form of delamination.
- Carbide-drill thrust force was found to be smaller than that of HSS drills, whereas the thrust force of the polycrystalline diamond drill was one third of that of the HSS drill.
- Conventional HSS tooling suffered the most wear and consequently produced a large increase in drilling forces. These higher forces in turn led to increased exit delamination and specimen damage. Tools with helical flutes were found to induce pulling thrust forces and entrance delamination, while those with straight flutes did not.

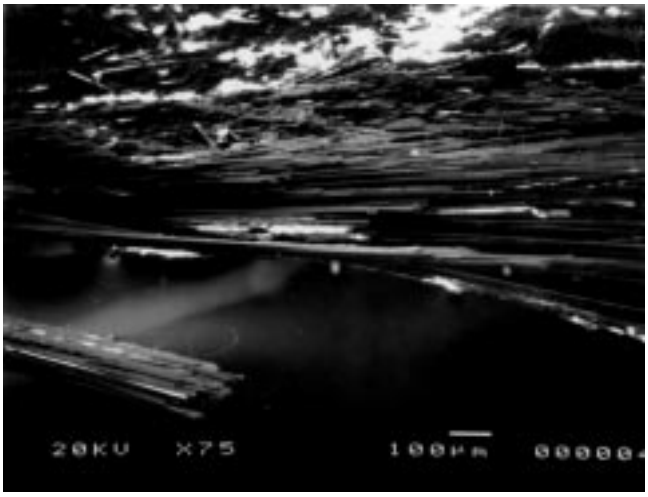

(a)

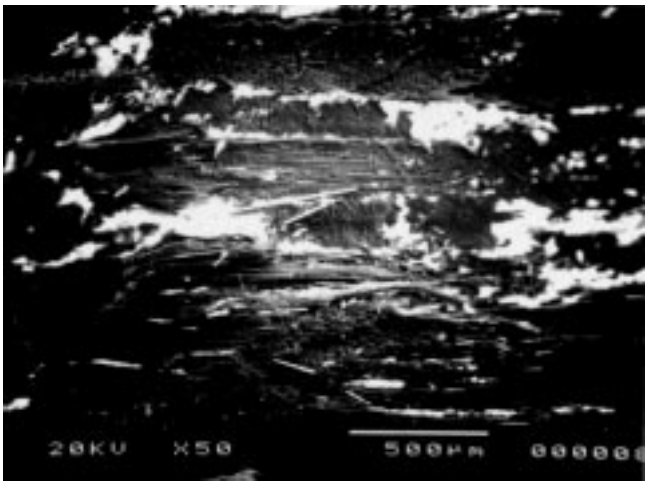

(b)

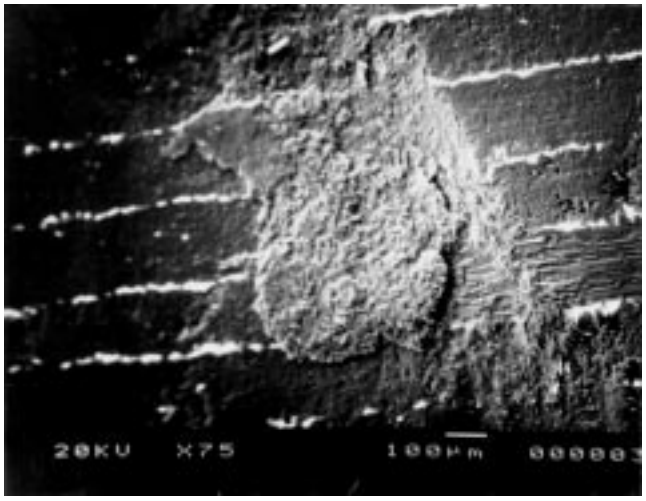

(c)

Fig. 11 SEM micrographs of the HSS drilled surface damage in graphite/bismaleimide (Gr/Bi) composite material. (a) Exit delamination. (b) Fiber fracture. (c) Matrix burning and smearing

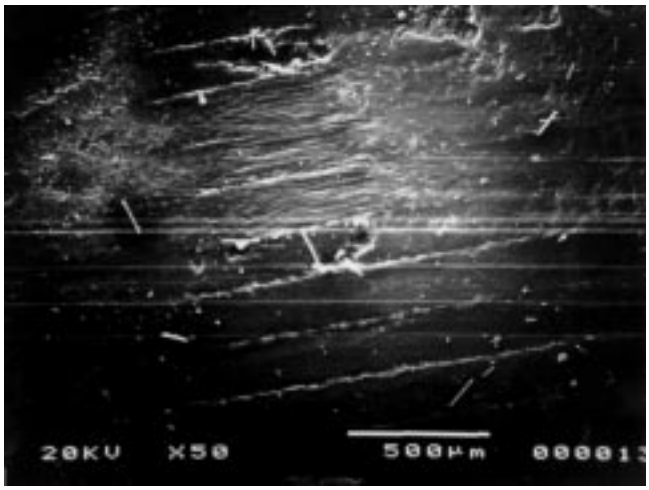

(a)

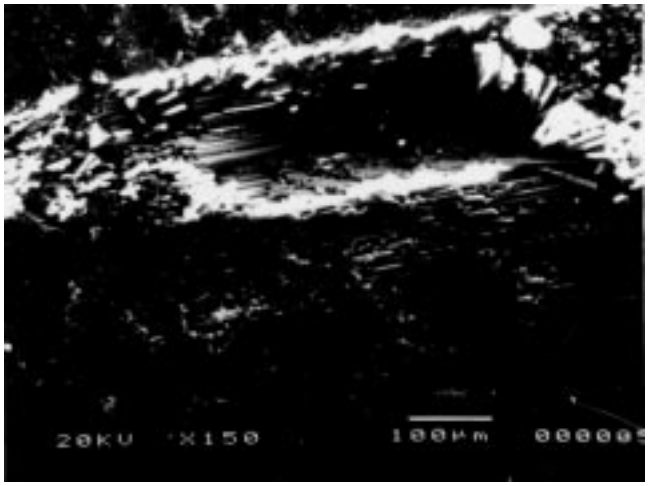

(b)

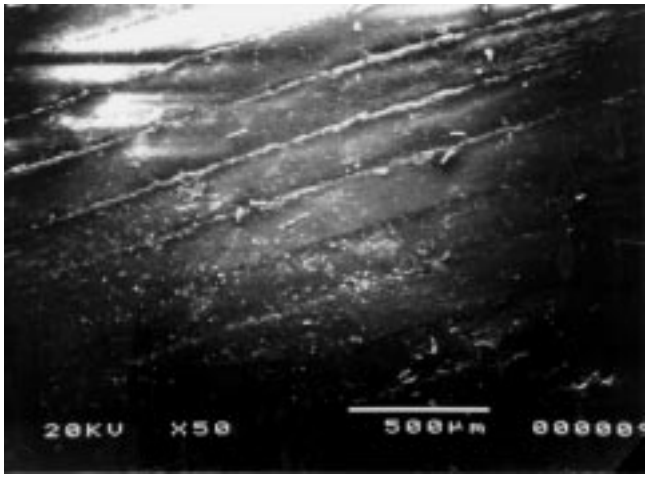

(c)

Fig. 12 SEM of drilled holes with different drilling tools. (a) Gr/Bi hole drilled with carbide tool. (b) Gr/Bi pitting with PCD tool. (c) Gr/Bi hole drilled with PCD tool

References

1. L. Colligan and M. Ramulu, The Effect of Edge Trimming on Composite Surface Plies, *Manuf. Rev.*, Vol 5 (No. 4), Dec 1992, p 274-283
2. W. Koing, Ch. Wulf, P. Crab, and H. Willerscheid, Machining of Fiber Reinforced Plastics, *Ann. CIRP,* Vol 34 (No. 2), 1985, p 537-548
3. S. Abrate and D.A. Walton, Machining of Composite Materials Part I: Traditional Methods, *Compos. Manuf.*, Vol 3 (No. 2), 1992, p 75-83
4. H. Ho-Cheng and C.H.K. Dharan, Delamination During Drilling in Composite Laminates, *J. Eng. Ind. (Trans. ASME),* Vol 112, 1990, p 236-239
5. A. Koplev, Cutting of CFRP with Single Edge Tool, *Proc. 3rd Mt. Conf. Comp. Mat.*, 1980 (Paris), p 1597-1605
6. D.H. Wang, M. Ramulu, and D. Arola, Orthogonal Cutting Mechanisms of Graphite/Epoxy Composite Part I: Unidirectional Laminate, *Int. J. Mach. Tools Manuf.*, Vol 35 (No. 12), 1995, p 1623-1638
7. D.H. Wang, M. Ramulu, and D. Arola, Orthogonal Cutting Mechanisms of Graphite/Epoxy Composite Part II: Multidirectional Laminate, *Int. J. Mach. Tools Manuf.*, Vol 35 (No. 12), 1995, p 1639-1648
8. D. Arola, M. Ramulu and D.H. Wang, Chip Formation in Orthogonal Trimming of Graphite/Epoxy Composites, *Compos. Part A: Appl. Sci. Manuf.*, Vol 27 (No. 2), 1996, p 121-133
9. T.L. Wong and S.M. Wu, An Analysis of Delamination in Drilling Composite Materials, *14th National SAMPE Technical Conference*, 1982, p 471-483
10. M. Ramulu, M. Faridnia, J.L. Garbini, and J.E. Jorgensen, Machining of Graphite/Epoxy Composite Material with Polycrystalline Diamond Tools, *J. Eng. Mater. Technol. (Trans ASME),* Vol 113 (No. 4), 1991, p 430-436
11. M. Ramulu, Characterization of PCD Inserts for Use in Machining Graphite/Epoxy Materials, "Mechanical Engineering Final Report to Boeing Advanced Systems," University of Washington, January 1989
12. M. Ramulu, J. Park, and D. Wang, PCD Cutter Evaluation, "Mechanical Engineering Final Report to Boeing Advanced Systems," University of Washington, May 1991
13. K. Colligan and M. Ramulu, An Experimental Investigation into Pitting of Hole Surfaces When Drilling Graphite/Epoxy Materials, MD-Vol 35, *Processing, Fabrication, and Manufacturing of Composite Materials*, ASME, 1992, p 11-25
14. S. Jain, D.C.H. Yang, Delamination-Free Drilling of Composite Laminates, MD-Vol 35, *Processing, Fabrication, and Manufacturing of Composite Materials*, ASME, 1992
15. J.A. Miller, Drilling Graphite/Epoxy at Lockheed, *Am. Mach. Autom. Manuf.*, October 1987
16. A. Dillio, V. Tagliaferri, and F. Veniali, Tool Life and Hole Quality in Drilling Aramid Composites, PD-Vol 37, *Composite Material Technology*, ASME, 1991
17. K. Sakuma, Y. Yokoo, and M. Seto, Study on Drilling of Reinforced Plastics (GFRP and CFRP): Relation between Tool Material and Wear Behavior, *Bull. JSME*, Vol 27 (No. 228), 1984, p 1237-1244
18. C.W. Wern, "Surface Characterization of Machined Graphite/Epoxy Composite," master's thesis, University of Washington, 1991